Orientation and interactions of dipolar molecules during transport through OmpF porin

Kindal M. Robertson, D. Peter Tieleman*

Department of Biological Sciences, University of Calgary, 2500 University Dr. NW, Calgary, AB, Canada T2N 1N4

Received 24 April 2002; revised 21 May 2002; accepted 24 July 2002

First published online 26 August 2002

Edited by Thomas L. James

Abstract **The outer membrane of Gram-negative bacteria contains porins, large sieve-like proteins allowing small molecules to diffuse in and out of the periplasm. We have simulated transport of the dipolar molecules alanine and methylglucose through the OmpF porin from *Escherichia coli* using non-equilibrium steered molecular dynamics simulations in a realistic bilayer environment. Structural perturbation of the protein is minimal. During the permeation process, both alanine and methylglucose align strongly in the electric field in the eyelet region, where the adhesion force on the permeating molecule has a maximum. Binding of the permeating dipolar molecules in the eyelet region is not observed.** **© 2002 Federation of European Biochemical Societies. Published by Elsevier Science B.V. All rights reserved.**

Key words: Non-equilibrium molecular dynamics; Sugar transport; Single molecule experiment; Alpha-methylglucose; Membrane protein; *Escherichia coli*

1. Introduction

Porins are passive diffusion pores from the outer membranes of Gram-negative bacteria [1,2]. OmpF is the major protein component of the outer membrane of *Escherichia coli* and is a non-specific pore that permits transport of ions and small molecules up to a mass of about 650 Da [3]. The structure of OmpF and a large number of mutants has been determined to high resolution, which makes this protein a prime target for understanding transport properties in porins and an ideal model system for computational methods to study transport and conductance [4–8]. One of the most conspicuous structural features of OmpF is the presence of an 'eyelet' region, a narrow site constricting the pore that is lined with charged residues. These residues would cause a strong transversal electric field, in addition to a screw-like field in the wider parts of the pore [4,5]. This feature is conserved in general diffusion porins and is therefore likely to be important physiologically [9,10]. Brownian dynamics simulations of ion flow through OmpF have shown that cations and anions follow distinct pathways with little overlap through the pore [5,11]. Several recent experiments on alpha-hemolysin [12,13] and maltoporin [14,15] have been able to probe permeation of individual molecules by electrophysiology techniques. This opens up exciting possibilities for experimental probing of permeation mechanisms as well as applications in using single molecule detection techniques. Computer simulations, with their atomic level of detail, can give unique additional information on the underlying motions of the channel protein and its interactions with the permeating molecules and have been used extensively to study ion transport [8]. In this letter, we consider the orientation and interaction of two dipolar molecules, alanine and alpha-methylglucose, as they move through the OmpF pore.

2. Materials and methods

The porin trimer was incorporated into a dimyristoylphosphatidylcholine bilayer using the procedure of Faraldo-Gomez et al. [16]. After insertion, the system was equilibrated for 100 ps using harmonic position restraints (1000 kJ mol^{-1} nm^{-2}) on all non-hydrogen atoms of the protein. The total system contained the porin, 337 united-atom DMPC lipids, 14434 water molecules, and 21 sodium ions (72157 atoms). Most amino acid pK_a values were adjusted according to the calculations of ref. [4], meaning Asp121, Asp127, Asp256, Asp312, Glu29, Glu296, Lys80 were uncharged. Arg82 was suggested to be uncharged by pK_a calculations but experimentally it has been determined that it is charged [9]. In the simulations Arg82 and also Arg167, in the barrel wall, were left in their default charged states. Starting from this pre-equilibrated system, alanine or alpha-methylglucose was placed near the extracellular end of each OmpF monomer. The resulting systems, called Ala and AMGL, respectively, were energy minimized to remove overlap between water and the newly introduced molecules. For both AMGL and Ala, a simulation of 1 ns was run with a 'spring' attached to the center of mass of alpha-methylglucose or alanine [17]. The spring force constant was 80000 kJ mol^{-1} nm^{-1}. This spring was pulled in the z-direction at a rate of 10^{-5} nm/step, or 5 nm in 1 ns. The extension of the spring in the z-direction gives the adhesion force in the z-direction through Hooke's law. A third simulation (Ala2) was performed with alanine molecules, in which the full side-chain charges in the eyelet region of OmpF were set to zero. Simulations used the GROMOS 43a2 forcefield [18] combined with lipid parameters from Berger et al. [19]. The temperature was controlled by the weak-coupling algorithm, separately for protein, lipid, and solvent plus ions with a time constant of 0.1 ps and a temperature of 300 K. The pressure was controlled by coupling of x, y and z separately to a pressure of 1 bar with a time constant of 1.0 ps [20]. A twin range cutoff of 0.9/1.4 nm was used for Van der Waals interactions, 0.9 nm and PME with a grid spacing of 0.12 nm and fourth order interpolation for electrostatics [21]. To allow a 5 fs timestep, polar hydrogen atoms in the protein were treated as dummy atoms with an increased mass of 4 Da, reconstructed every step assuming an ideal geometry based on the positions of the neighboring heavy atoms [22] and the stable LINCS algorithm was used to constrain bond lengths and angles involving hydroxyl groups [23]. It has been shown that this method does not significantly affect the accuracy of the simulation [22,24]. Simulations were done with the GROMACS package [25,26] (http://www.gromacs.org).

*Corresponding author. Fax: (1)-403-289 9311.
E-mail address: tieleman@ucalgary.ca (D.P. Tieleman).

PII: S0014-5793(02)03173-3

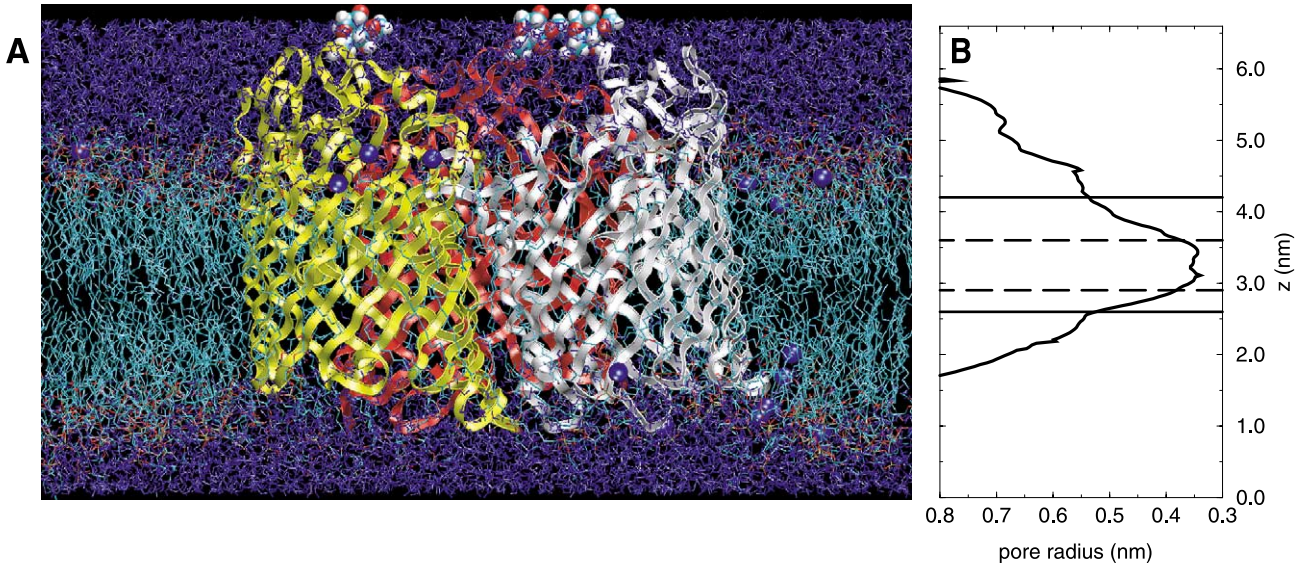

Fig. 1. A: Side view of the simulation system. The porin trimer is shown schematically, the three AMGL molecules and sodium ions as space filling, water and lipids as lines. The z-axis is normal to the membrane and coincides with the symmetry axis of the porin trimer. B: Pore radius profile of an OmpF monomer (calculated from the starting structure, with a spherical probe using HOLE [31]). The intracellular side is down ($z = 0$ nm), the extracellular side up ($z = 6$ nm). Molecules are pulled from a z-coordinate of 6.5 to 1.5 nm.

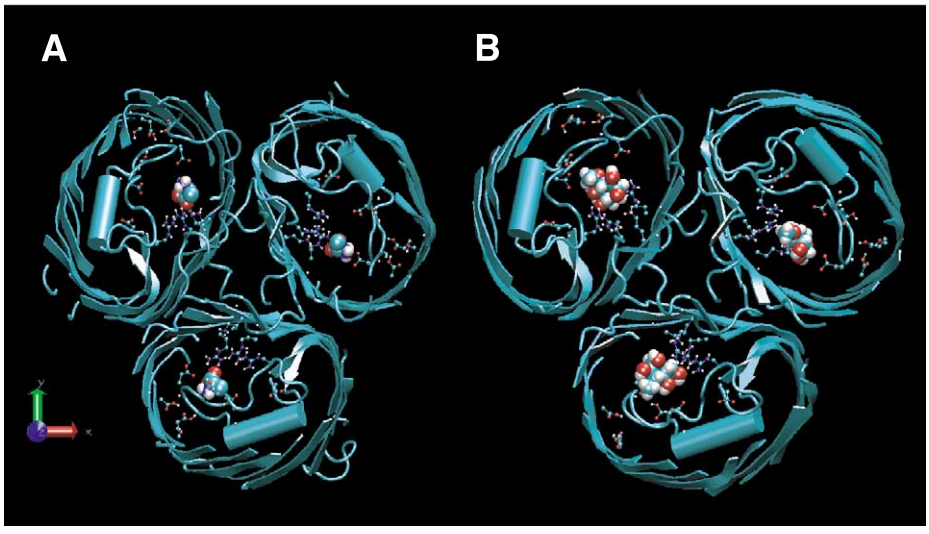

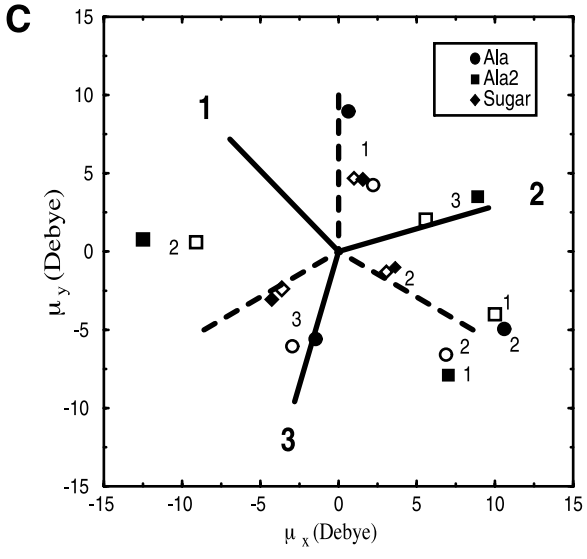

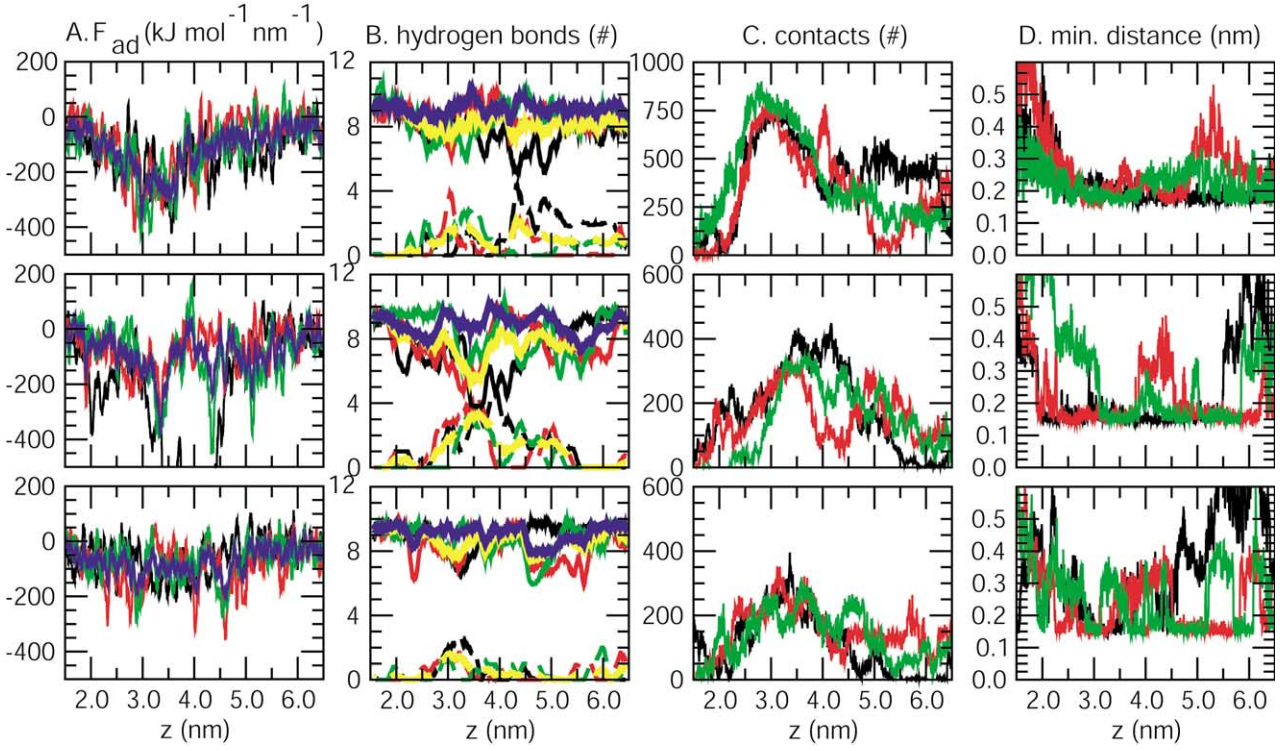

Fig. 3. Characteristic properties during permeation of alpha-methylglucose (top row), alanine (middle row) and alanine in Ala2 (bottom row). In all cases, black, red and green represent the individual permeating molecules. Data have been averaged over 2.5 ps. A: Adhesion force profiles. The blue lines is the adhesion force averaged over three molecules; B: number of hydrogen bonds between permeating molecule and water (solid lines) and OmpF (dashed lines). Yellow is the average of the three, blue the total number of hydrogen bonds with the permeating molecule; C: number of OmpF atoms within 0.6 nm of the permeating molecule; D: minimum distance between any atom of the permeating molecule and any OmpF atom.

3. Results and discussion

Fig. 1 shows a snapshot of the simulation system and the pore radius profile for a single monomer. Clearly, between ca. 3.0 and 3.5 nm the pore narrows to a radius of about 0.35 nm. In Fig. 2, snapshots from the simulations are shown, between 2.6 and 4.2 nm, with permeating alpha-methylglucose and alanine molecules. Alanine, with a molecular mass of 89 Da, is considerably smaller than alpha-methylglucose (194 Da). The snapshots of Ala suggest strong interactions between the charged termini and the charged residues in the eyelet region. The sugars also have a significant orientation. To quantify this observation, the dipole moment vectors projected on the x,y plane for all three molecules in the three simulations are plotted in Fig. 2. These projections give a numerical estimate of the degree of orientation. The solid lines bisect the pore in the eyelet region in each of the three monomers. The direction of the transversal field in the eyelet region is at an angle with these solid lines. Both sugar and alanine align strongly with the transversal field, although there is some variation in the degree of orientation. The dashed lines indicate approximately the orientation of the permeating molecules and the direction of the transversal field. As a control, Ala2 (with no charges on the protein residues in the eyelet region) shows no correlation with the protein structure. It is interesting to note that in a previous simulation, a strong ordering of water molecules and a significantly reduced diffusion coefficient in the narrow parts of the pore were observed [7]. In the OmpF crystal structure, bound water molecules in the pore are observed too, but because of the resolution of the crystal structure their orientation could not be determined [3]. Fig. 2 only shows the average orientation in the eyelet region. An analysis of the orientation of the permeating molecules in the wider regions of the pore did not show the screw-like behavior calculated from continuum calculations [4,5] (data not shown). Previous molecular dynamics simulations have shown in detail the complex shape of the electric field in the wider parts of the porin based on water orientation [7]. The electric field in these parts however is not as strong as in the eyelet region, and many permeation pathways are possible.

←

Fig. 2. A,B: Snapshots of the structure in the constriction zone: Ala (A) and AMGL (B). A slice between 2.0 and 4.5 nm has been cut from the full structure and only porin and permeating molecules are shown. In both cases, the center of mass of the permeating molecules is at 3.2 nm, the narrowest part of the pore. Figure was made with VMD [32]. C: Dipole projections on the x,y plane averaged over 2.6–4.2 nm (open symbols) and over 2.8–3.6 nm (closed symbols). See the pore radius profile in Fig. 1 for the two regions. The x- and y-axes correspond to the axes in A and B. The large numbers 1–3 indicate the three monomers, the small numbers 1–3 indicate the three permeating molecules corresponding to monomers 1–3. The solid lines, based on the crystal structure, approximately bisect the pore opening. The dashed lines only indicate the approximate three-fold symmetrical arrangement of the dipole projections.

The sampling of these paths in the present simulations may be insufficient.

In Fig. 3, a more numerical view of the permeation process is shown, summarizing the adhesion forces on the permeating molecules and the interactions between the permeating molecules and the porin. Initially, the sugar or alanine molecules are placed at 6.5 nm, near the extracellular side of the porin. Over the course of 1 ns, they are pulled through the porin, to the intracellular side. The pore radius profile (Fig. 1B) shows that the most constricted part of the pore lies between ca. 3.0 and 3.5 nm. In Fig. 3A, the adhesion force each of the molecules experiences while being pulled through the pore is plotted as a function of location in the pore. In the wider parts of the channel the adhesion force fluctuates heavily but is close to zero on average. The three alpha-methylglucose molecules experience a very similar force with a clear maximum in its magnitude in the narrowest part of the pore between 3.0 and 3.5 nm. In Ala and Ala2, the forces are comparable outside the narrow part of the pore, except for the one outlier (black line in Ala). In the eyelet region however, the adhesion forces are much larger in Ala than in Ala2, indicative of the important role of electrostatic interactions in the eyelet region.

What determines the adhesion force during permeation? Fig. 3B–D shows the number of hydrogen bonds between the permeating molecule and the porin or solvent, the minimum distance between the permeating molecules and the porin, and the number of porin atoms within a 0.6 nm radius of the permeating molecules. Outside of the eyelet region, the sugar molecules form hydrogen bonds with water and very little with the porin. As the pore narrows, all three sugar molecules increase the number of hydrogen bonds with OmpF. Between 4 and 6 nm, the number of water molecules varies due to the different paths the three sugars take through the wide part of the pore. The same picture emerges from the number of contacts between the sugars and OmpF and the minimum distance: in the narrow part of the pore all three sugars show comparable interactions, whereas in the wider part different paths are followed. The minimum distance is approximate 0.18 nm, corresponding to hydrogen bonds. In Ala, there are comparatively more interactions between OmpF and alanine than OmpF and alpha-methylglucose, which is likely due to the high charges on the alanine. The minimum distance in the center of the pore corresponds to salt bridge formation with charged residues in the eyelet region, although different residues are involved for individual permeating molecules. When the charges near the eyelet region of the porin are removed, alanine has less tendency to interact with the porin and less hydrogen bonds between porin and alanine are formed. The minimum distance in the narrowest part of the channel in this case is less reproducible between the three molecules and corresponds to interactions between the charged termini and polar atoms in the porin. In all cases, the total number of hydrogen bonds formed by permeating molecules is approximately constant.

It is useful to consider some of the limitations of the simulation. The most serious approximation is the short time scale, or the fast rate at which molecules are pulled through the porin. One outlier in the case of Ala has such a large force that its path will be physically unrealistic. Nonetheless, the sugars in particular show the same adhesion force profile, despite being independent and having different initial orientations and motion in the x,y directions during permeation. Analysis of hydrogen bonding, minimum contact distances and the number of OmpF atoms in a 0.6 nm radius from the permeating molecules also suggest that in the narrow part of the channel in each of the three monomers the permeating molecules show the same behavior, suggesting that the results are reproducible. Differences in the wider part are to be expected, because the wide pores allow different paths for permeating molecules. A second approximation is the possibly reduced degree of screening of the interactions of permeating dipolar molecules and the charged residues lining the pore because the simulations do not include salt solution. This effect has been partially incorporated by changing the pK_as of amino acids depending on the local electric field, but some degree of approximation remains involved. The weakly dipolar alpha-methylglucose is less likely to be affected by this.

Why do OmpF and other general diffusion porins have clearly separated clusters of charge in the narrowest part of the pore [9,10]? It might not seem to be favorable for the important function of transport of dipolar molecules, because a strongly dipolar molecule with a size comparable to the pore might bind and block the pore. The simulations suggest that this is not the case. The integrated adhesion force curves give the adhesion energy, which is similar to a free energy profile except for a significant contribution from friction due to the high pull rate. This irreversible work component is the reason why there is a difference in free energy between both sides of the bilayer in the simulation. The adhesion energy profile (graph not shown) does not have a clear minimum in the pore, which would correspond to binding in the eyelet region. Such a minimum would be seen in the adhesion force profile as a change in sign of the adhesion force beyond the eyelet, acting to move the molecule back into the eyelet region. This suggests that alpha-methylglucose and alanine do not show a tendency to bind in the eyelet region, in spite of their dipole moments. This could, e.g. be due to unfavorable entropic factors, or the shape of the electric field outside the eyelet region. Detailed free energy calculations could address this suggestion, but unfortunately for a system this size this is not yet feasible. Many charged (zwitterionic) substrates such as amino acids are small and compete with ions for interactions in the pore, thus preventing binding. Interestingly, the still unresolved question of the importance of voltage gating in OmpF and related general diffusion porins may also hinge on the charges near the eyelet region [27–30]. While the charge clusters allow efficient transport of anions and cations as well as dipolar molecules, an understanding of the physiological role of voltage gating might be required to complete the picture.

4. Conclusion

We have shown that non-equilibrium molecular dynamics simulations can give reproducible results for the transport of alpha-methylglucose and alanine through OmpF porin. Such simulations may be generally useful for characterizing in atomic detail transport of small molecules and help interpret single channel experiments on binding and permeation of small molecules. The dipolar molecules alpha-methylglucose and alanine align strongly in the transversal field in the narrowest part of OmpF, where they experience the maximum adhesion force. No clear binding of the molecules in the eyelet region is observed.

Acknowledgements: D.P.T. is a Scholar of the Alberta Heritage Foundation for Medical Research. This work was sponsored in part by Project Cybercell™.

References

[1] Schulz, G.E. (1996) Curr. Opin. Struct. Biol. 6, 485–490.
[2] Nikaido, H. (1994) J. Biol. Chem. 269, 3905–3908.
[3] Cowan, S.W., Schirmer, T., Rummel, G., Steiert, M., Ghosh, R., Pauptit, R.A., Jansonius, J.N. and Rosenbusch, J.P. (1992) Nature 358, 727–733.
[4] Karshikoff, A., Spassov, V., Cowan, S.W., Ladenstein, R. and Schirmer, T. (1994) J. Mol. Biol. 240, 372–384.
[5] Schirmer, T. and Phale, P.S. (1999) J. Mol. Biol. 294, 1159–1167.
[6] Im, W., Seefeld, S. and Roux, B. (2000) Biophys. J. 79, 788–801.
[7] Tieleman, D.P. and Berendsen, H.J.C. (1998) Biophys. J. 74, 2786–2801.
[8] Tieleman, D.P., Biggin, P.C., Smith, G.R. and Sansom, M.S. (2001) Q. Rev. Biophys. 34, 473–561.
[9] Schirmer, T. (1998) J. Struct. Biol. 121, 101–109.
[10] Koebnik, R., Locher, K.P. and Van Gelder, P. (2000) Mol. Microbiol. 37, 239–253.
[11] Phale, P.S., Philippsen, A., Widmer, C., Phale, V.P., Rosenbusch, J.P. and Schirmer, T. (2001) Biochemistry 40, 6319–6325.
[12] Gu, L.Q., Braha, O., Conlan, S., Cheley, S. and Bayley, H. (1999) Nature 398, 686–690.
[13] Bayley, H. and Cremer, P.S. (2001) Nature 413, 226–230.
[14] Bezrukov, S.M., Kullman, L. and Winterhalter, M. (2000) FEBS Lett. 476, 224–228.
[15] Kullman, L., Winterhalter, M. and Bezrukov, S.M. (2002) Biophys. J. 82, 803–812.
[16] Faraldo-Gómez, J.D., Smith, G.R. and Sansom, M.S.P. (2002) Eur. Biophys. J. 31, 217–227.
[17] Isralewitz, B., Gao, M. and Schulten, K. (2001) Curr. Opin. Struct. Biol. 11, 224–230.
[18] van Gunsteren, W.F., Kruger, P., Billeter, S.R., Mark, A.E., Eising, A.A., Scott, W.R.P., Huneberger, P.H. and Tironi, I.G. (1996) The GROMOS96 Manual and User Guide, Biomos and Hochschulverlag AG an der ETH Zurich, Groningen.
[19] Berger, O., Edholm, O. and Jahnig, F. (1997) Biophys. J. 72, 2002–2013.
[20] Berendsen, H.J.C., Postma, J.P.M., van Gunsteren, W.F., DiNola, A. and Haak, J.R. (1984) J. Chem. Phys. 81, 3684–3690.
[21] Essmann, U., Perera, L., Berkowitz, M.L., Darden, T., Lee, H. and Pedersen, L.G. (1995) J. Chem. Phys. 103, 8577–8593.
[22] Feenstra, K.A., Hess, B. and Berendsen, H.J.C. (1999) J. Comp. Chem. 20, 786–798.
[23] Hess, B., Bekker, H., Berendsen, H.J.C. and Fraaije, J.G.E.M. (1997) J. Comp. Chem. 18, 1463–1472.
[24] Tieleman, D.P., Berendsen, H.J.C. and Sansom, M.S.P. (2001) Biophys. J. 90, 331–346.
[25] Lindahl, E., Hess, B. and Van der Spoel, D. (2001) J. Mol. Model. 7, 306–317.
[26] Berendsen, H.J.C., Van der Spoel, D. and Van Drunen, R. (1995) Comp. Phys. Comm. 91, 43–56.
[27] Samartzidou, H. and Delcour, A.H. (1998) EMBO J. 17, 93–100.
[28] Van Gelder, P., Dumas, F. and Winterhalter, M. (2000) Biophys. Chem. 85, 153–167.
[29] Van Gelder, P., Saint, N., Phale, P., Eppens, E.F., Prilipov, A., van Boxtel, R., Rosenbusch, J.P. and Tommassen, J. (1997) J. Mol. Biol. 269, 468–472.
[30] Robertson, K.M. and Tieleman, D.P. (2002) Biochem. Cell. Biol. 80(5), in press.
[31] Smart, O.S., Neduvelil, J.G., Wang, X., Wallace, B.A., Sansom, M.S. (1996) J. Mol. Graph. 14, 354–60, 376.
[32] Humphrey, W., Dalke, A. and Schulten, K. (1996) J. Mol. Graph. 14, 33–8, 27–8.